

## Seismic evaluation of existing RC frames with wide beams using an energy-based approach

A. Benavent-Climent\* and R. Zahran

*Department of Structural Mechanics, University of Granada, Edificio Politécnico, 18071 Granada, Spain*

(Received December 8, 2009, Accepted February 20, 2010)

**Abstract.** This paper investigates the seismic performance of existing reinforced concrete frames with wide beams mainly designed for gravity loads, as typically found in the seismic-prone Mediterranean area before the introduction of modern codes. The seismic capacity is evaluated in terms of the overall amount of input energy that the frame can dissipate/absorb up to collapse. This approach provides a quantitative evaluation that can be useful for selecting and designing an appropriate retrofit strategy. Six prototype frames representative of past construction practices in the southern part of Spain are designed, and the corresponding non-linear numerical models are developed and calibrated with purposely conducted tests on wide beam-column subassemblages. The models are subjected to sixteen earthquake records until collapse by applying the incremental dynamic analysis method. It is found that the ultimate energy dissipation capacity at the story level is markedly low (about 1.36 times the product of the lateral yield strength and yield displacement of the story), giving values for the maximum amount of energy that the frame can dissipate which are from one fourth to half of that required in moderate-seismicity regions.

**Keywords:** seismic performance; existing frames; energy dissipation capacity; wide beams.

### 1. Introduction

Many existing moment-resisting frame structures, designed with substandard details or inadequate antiseismic criteria following past seismic codes, were seen to collapse or undergo severe damage in recent earthquakes such as Kokaeli in Turkey (1999), Chi-chi in Taiwan (2001) or the more recent in L'Aquila in Italy (2009). In the future, very dangerous consequences of earthquakes are likely to come from this type of existing buildings. Extensive experimental-analytical research has been carried out in recent years on the seismic performance of existing reinforced concrete (RC) frames mainly designed for gravity loads (Aycardi *et al.* 1994, Beres *et al.* 1996, Hakuto *et al.* 2000, Bing *et al.* 2002, Calvi *et al.* 2002, Park 2002, Benavent-Climent *et al.* 2004, Masi 2004). Such studies have confirmed the expected inherent weaknesses of these systems, which are mainly a consequence of poor reinforcement detailing, a lack of transverse reinforcement in the joint region, and the absence of any capacity design principles. These weaknesses result in brittle failure mechanisms either at the local level (e.g., shear failure in the joints, columns or beams) or the global level (e.g., soft story mechanism). Exterior beam-column joints are particularly vulnerable, due to the intrinsic lack of alternative and reliable sources to transfer shear within the panel zone region after cracking.

\* Corresponding author, Professor, E-mail: benavent@ugr.es

Past research on existing gravity-load designed structures has focused on the RC frames with “normal” beam-column connections, that is, those in which the depth of the beam  $h_b$  is larger than its width  $b_b$ , and  $b_b$  is equal to or smaller than the width of the column  $b_c$ . Counterpart studies on frames with wide beam-column connections are comparatively very limited, since this type of construction is less prevalent than normal connections, except in the moderate-seismicity Mediterranean area (Spain, Italy, etc.). RC frames with wide beam-column connections and one-way slabs are structural systems in which the slab is constructed with joists from which the load is transferred to shallow beams whose width  $b_b$  exceeds the width of the column  $b_c$ , and whose depth  $h_b$  is equal to the thickness of the joist (typically 200-300 mm). They are commonly called banded-floor systems or wide-beam systems and can be thought of as part way between normal beam-column connections and flat-plate to column connections. Wide beams have been intensively used in the Mediterranean area as a primary gravity load-carrying system because they allow more flexibility in the definition of spaces, and they are very effective in reducing the formwork. However, they present several drawbacks when used in seismic regions as a lateral load-resisting system: (i) a deficient transfer of the bending moment from the wide beam to the column; (ii) a low lateral stiffness; and (iii) a poor energy dissipation capacity. These drawbacks owe primarily to the fact that part of the wide beam longitudinal reinforcement is anchored in transverse beams perpendicular to the wide beams and adjacent to the column, rather than in the column core.

This paper reports on a numerical study intended to evaluate the seismic performance of existing frames with wide beam-column connections, built during the 70's and 80's in the Mediterranean area (Spain) according to old seismic codes. These codes did not pay attention to ductility issues either at the local level (i.e., poor reinforcement detailing, absence of capacity design principles, etc.), or global level (i.e., lack of design considerations oriented to form strong column-weak beam plastic mechanisms). In previous research, the seismic performance of existing structures was evaluated mainly in terms of local ductility demands, damage indexes and maximum inter-story drift induced in the frame under a given earthquake. However, studies regarding the estimation of the ultimate energy absorption/dissipation capacity, UEDC, are almost nonexistent. Quantitative comparison of the UEDC of an existing frame with the seismic energy input demand expected at the site can provide valuable information about the proneness of the building to collapse, and it can also orient decisions regarding the most appropriate approach to retrofit the structure.

## **2. Procedure**

The seismic evaluation of existing frames belonging to a particular structural typology involves several steps:

- 1) Selecting typical configurations of the structural typology during the period under study;
- 2) Designing reference structures on the basis of codes and current practices of the period;
- 3) Developing realistic non-linear numerical models representative of the reference structures;
- 4) Selecting a set of accelerograms;
- 5) Calculating the seismic response through non-linear dynamic analysis; and,
- 6) Evaluating the response in terms of ductility demands, damage indexes, maximum inter-story drifts, energy dissipation demands, etc.

Hereafter, the above steps are particularized to the structural type under study, with a focus on evaluating the seismic response at the ultimate state in terms of dissipated energy.

## 2.1 Selection of reference models of the structural type

Most existing buildings with RC frames constructed during the 70's and 80's of the 20th century in the southern part of Spain are residential constructions with wide beam systems designed under the former Spanish seismic code PDS-74, which prescribed lateral loads smaller than the current code and did not provide any requirement for attaining ductility. Based on a field survey, the provisions of the earlier seismic code PDS-74, and the review of construction practices at that time, six reference buildings were designed by combining the typically observed number of stories  $N$  ( $=3, 5, 6$  and  $8$ ), the span in the direction of the wide beams  $l$  ( $=3.5, 4.5, 5, 5.5$  and  $6$  m), the span perpendicular to the wide beams  $l'$  ( $=5$  m and  $5.5$  m), and the wide-beam depth  $h_b$  ( $=0.27$  m and  $0.30$  m). Typical interstory heights of  $2.8$  and  $4.5$  m for the first floor, and  $2.8$  and  $3$  m for the upper stories were adopted. One plane frame was selected from each building and referred to as model N3S4, N5S2, N5S3, N6S4, N8S2 or N8S3, as shown in Fig. 1. All were interior frames, except the one obtained from the building with  $N=3$ ,  $l=l'=5$  m and  $h_b=0.27$  m (model N3S4), which was an exterior frame. The contribution of the infills of the exterior frames to the strength and stiffness were neglected. Neglecting this contribution provides an evaluation of the seismic capacity of the structure that is on the safe-side because, since there is no gap between the infill and the frame, there might be a significant effect for small drift levels. However, quantifying this effect in old

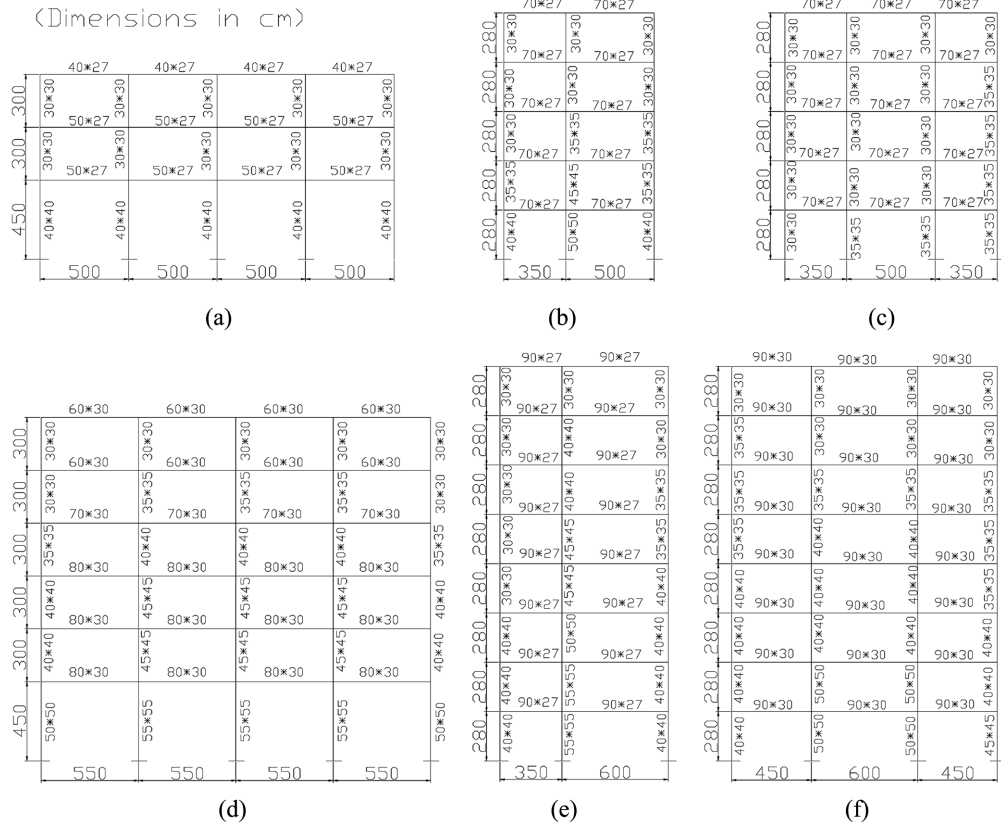


Fig. 1 Typical reference frames (a) N3S4, (b) N5S2, (c) N5S3, (d) N6S4, (e) N8S2, (f) N8S3

buildings is very difficult. The interior and central frames typically have very thin partitions (4-7 cm thick) made of hollow bricks, with openings for doors, and mostly not contained in the plane of the frames; their contribution to the seismic resistance was also neglected. Neglecting the infills makes the results of the analyses partially representative of the RC built environment.

## *2.2 Structural design of the reference models*

The values of the dead ( $4.25 \text{ kN/m}^2$ ), live ( $3 \text{ kN/m}^2$ ) and seismic loads prescribed by Spanish codes during the period of construction of the buildings were used to design the models. The frames were assumed to be located on stiff soil in the southern part of Spain (Granada region), where the design peak ground acceleration (PGA) prescribed by the current seismic code is  $0.23\text{g}$ . The design lateral earthquake loads consisted of an inverted triangular distribution, and the base shears normalized by the total building weight ranged between 0.10 and 0.28. Concrete with compressive strength  $f_c=17.5 \text{ MPa}$  and deformed steel with yield stress  $f_y=400 \text{ MPa}$  were assumed;  $f_c$  and  $f_y$  represent characteristic values of the corresponding quantities. Criteria and non-ductile details used in the construction practice over twenty years ago in Spain were taken into account in designing the RC members. Accordingly, the reference models have in common the following features: (i) the members are rather slender with low amounts of longitudinal reinforcement; (ii) about one half of the longitudinal reinforcement of the wide beam is anchored outside the column core; (iii) the amount of longitudinal reinforcement is different at the top and at the bottom of the wide beam; (iv) the shear reinforcement is governed by the gravity loads resulting in light transverse reinforcement in columns – 6 mm bars spaced 0.25-0.3 m – and an adequate amount of stirrups in beams – 6-8 mm bars spaced 0.10-0.15 m.

## *2.3 Numerical modeling for dynamic analysis*

Six numerical models intended to represent the frames of Fig. 1 in a sufficiently reliable way – in terms of stiffness, strength and ultimate energy dissipation capacity – were developed by using the IDARC-2D code (Park *et al.* 1987). The hysteretic modeling of RC members took into account that the structures had medium-good construction characteristics.

For realistically modeling the behavior of the wide beams, the results of prior static tests (Benavent-Climent *et al.* 2009a, b) on two 2/3-scale exterior and two interior wide-beam column connections representing the construction practices in Spain during the 1970's and 1980's were used. These results are consistent with those obtained from dynamic tests by the first author (Benavent-Climent 2005, 2007). In the tests conducted by Benavent-Climent *et al.* (2009a, b), the columns remained almost elastic and the failure mechanism was governed by the flexural yielding of the wide beams. Similar to the behavior reported for old Italian RC buildings, shear, bond or joint failures were not observed. The connections were tested until failure, which was assumed to occur when the strength degraded below 0.75%  $Q_{max}$ , where  $Q_{max}$  is the maximum strength reached during the test. The corresponding chord rotation ductility ratio was 2.8 for the wide beams in the interior connections, and 2.1 for the wide beams of the exterior connections. The total amount of plastic strain energy dissipated by each wide beam until failure, normalized by  $Q_{max} \times \delta_y$ , was 9 for the wide beams in interior connections, and 4 for the wide beams in exterior connections. Here,  $\delta_y$  is the yield displacement corresponding to  $Q_{max}$ . The cyclic behavior of the wide-beams observed in the tests was idealized with the polygonal hysteretic model (PHM) implemented in IDARC. Consistent

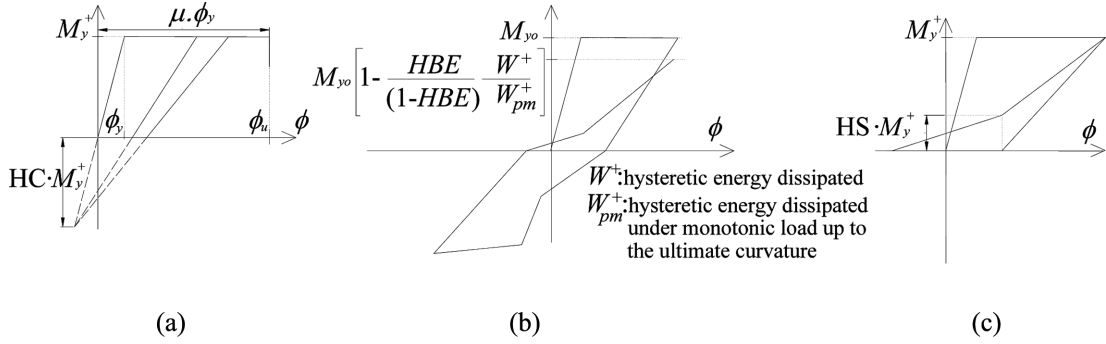


Fig. 2 Hysteretic parameters of RC members (a) HC and \$\mu\$, (b) HBE, (c) HS

with the test results, only the flexure failure mode in beams was considered. The PHM model is an extension of the three-parameter Park model; it uses a non-symmetric monotonic envelope defined by the secant stiffness  $K_o$ , the yielding moment  $M_y$ , the curvature-ductility factor  $\mu$ , and four parameters that control the effects of stiffness degradation (HC), strength degradation (HBE, HBD) and pinching (HS). The meaning of HC, HBE and HS is illustrated in Fig. 2 (Park *et al.* 1987, Sivaselvan and Reinhorn 1999). HBD is not used in this study since it is made equal to 0. The secant stiffness  $K_o$  was calculated multiplying the initial elastic stiffness of the uncracked gross sections by a factor  $\gamma$  (Sugano 1968), given by

$$\gamma = \left[ 0.043 + 1.6n \frac{a_t}{bh} + 0.043 \frac{a}{h} + 0.33 p_o \right] \left( \frac{d}{h} \right)^2 \quad (1)$$

Here,  $n$  is the ratio between the Young modulus of steel and concrete;  $a_t$  is the area of the longitudinal tension bars;  $b, h$  are the width and depth of the section;  $p_o = P/(hbf_c)$  is the ratio of the axial load  $P$  (positive in compression),  $d$  is the effective depth and  $a$  is the shear span.

The yield moment  $M_y$  of the wide-beams was calculated following the approach proposed by Benavent-Climent *et al.* (2009a, b), which takes into account the amount of longitudinal reinforcement anchored outside the column core, and the fact that the flexural capacity of the wide beam is limited by the torsion capacity of the transverse beams. The parameters  $\mu$ , HC, HBE and HS were calibrated through a parametric study on the basis of the experimental results (Benavent-Climent *et al.* 2009a, b), giving HS=0.2,  $\mu=12$ , HC=2, HBE=0.6 for wide-beams in exterior connections; and HS=0.2,  $\mu=21$ , HC=3.5, HBE=0.4 for wide beams in interior connections. These values of the curvature ductility  $\mu$  are similar to those adopted by Masi (2004) for flexible beams of post-1970 Italian RC frames ( $\mu=20$ ), and they provide chord rotation ductility ratios close to those obtained in the tests. For the purpose of illustration, Fig. 3 compares experimental and simulated hysteretic curves.

The design of the columns was governed by the gravity loads, without considering ductile provisions of modern seismic codes. Typical column details include: (i) hook extensions shorter than the lengths specified in current codes; (ii) light transverse reinforcement – 6-10 mm diameter column ties spaced 250-300 mm; (iii) longitudinal reinforcement lap splices just above the floor level, with lengths of about 25 times the diameter of the longitudinal bar; and (iv) medium quality concrete. The PHM model employed for the wide beams was used also for modeling the hysteretic behavior of column sections; the calibration of parameters HS,  $\mu$ , HC, HBE was based on the

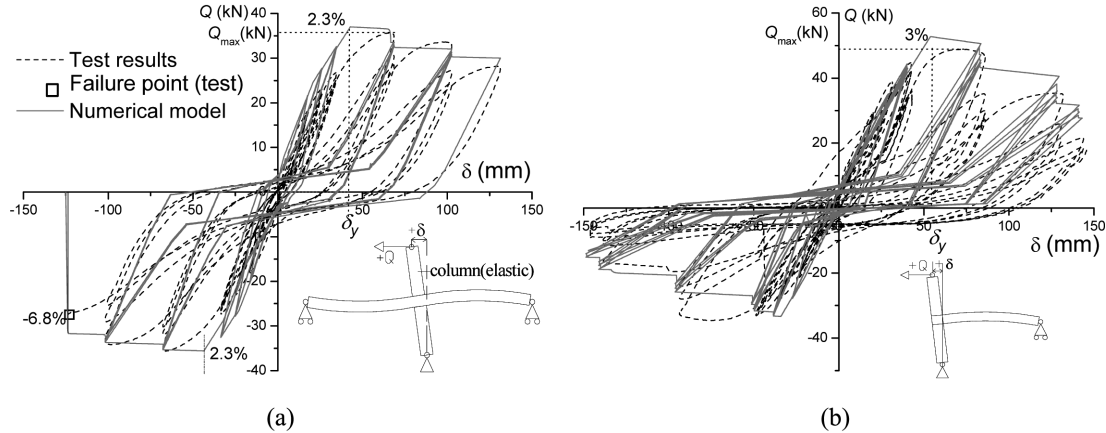


Fig. 3 Comparison between test results and simulation (a) interior beam, (b) exterior beam

results of the experiments conducted by Sezen and Moehle (2006), giving  $\mu=3$ , HS=0.2, HC=2.5 and HBE=0.5. These authors tested four columns typical of old frames designed for gravity loads and found that even in those that yielded in flexure, brittle shear failure occurred after the flexural strength was reached limiting the chord rotation ductility to values ranging between 1.29 and 3.14. Accordingly, only shear failure mode was considered in columns for the study presented here. It is worth noting that the axial load ratio of two of the columns tested by Sezen and Moehle (2006) was 0.15, and that of the other two 0.60. Although the large difference in the axial load ratios of the two pairs of columns, they exhibited similar ductilities:  $\mu=3.01$  and  $\mu=2.34$ . Similarly to the wide beams, the secant stiffness  $K_o$  was calculated by multiplying the initial elastic stiffness of the uncracked gross section of the column by the factor  $\gamma$  given by Eq. (1). The flexural and shear capacities of the columns were estimated using the formulae of the Japanese standard for evaluation of seismic capacity of existing RC buildings. It is worth noting that, according to Priestley (1997),  $\mu=3$  is the value of the curvature ductility at which the concrete shear strength in columns starts to decrease sharply. The masses of the numerical models consisted of the dead load plus 30% of the

Table 1 Modal properties of the frames investigated ( $T_I$  in s;  $M_T$  in  $kNs^2/mm$ )

N	N3S4	N5S2	N5S3	N6S4	N8S2	N8S3
	$T_I=1.40$	$T_I=1.23$	$T_I=1.75$	$T_I=1.82$	$T_I=2.26$	$T_I=1.94$
	$M_I=0.2219$	$M_I=0.1183$	$M_I=0.2314$	$M_I=0.5302$	$M_I=0.2987$	$M_I=0.4351$
	$m_I=87\%$	$m_I=77\%$	$m_I=73\%$	$m_I=83\%$	$m_I=76\%$	$m_I=78\%$
	$\phi_1$	$\phi_1$	$\phi_1$	$\phi_1$	$\phi_1$	$\phi_1$
8					1	1
7					.93	.92
6				2.02	.83	.81
5		1	1	1.77	.71	.68
4		.84	.86	1.44	.55	.54
3	2.84	.58	.63	1.11	.39	.38
2	2.12	.35	.39	0.78	.23	.22
1	1.00	.15	.17	0.41	.09	.09

live load. In addition to energy dissipation due to hysteresis, a  $\xi=0.05$  ratio of viscous damping was included. This value takes into account that the infills are able to dissipate some energy, though in this study they were considered ineffective in sustaining seismic loads, as pointed out above. Table 1 summarizes the period  $T_1$  and modal shape  $\phi_1$  of the first vibration mode, together with the total mass  $M_T$  of each frame under study and the mass percentage of the first mode  $m_1$ .

## 2.4 Seismic input

Sixteen natural earthquakes drawn from the European Strong Motion Database (Ambraseys *et al.* 2004) were used for the inelastic time-history analyses, as shown in Table 2. The Table shows the fault distance, i.e., the shortest distance to the surface projection of the rupture surface or Joyner-Boore distance, and the epicentral distance. Records with distances less than 10 km were not included in order to avoid effects of directivity from near field sources. Only the horizontal components were considered.

## 2.5 Incremental dynamic analysis

To investigate the seismic capacity of the structural typology under study, the incremental nonlinear dynamic analysis (IDA) method is used (Vamvatsikos and Cornell 2002). Accordingly, the frames are subjected to the ground motion records of Table 2, each scaled to multiple levels of intensity. A scale factor  $\lambda$  is applied to the ground acceleration record starting from  $\lambda=0$ , and it is increased progressively until the structure reaches the target limit state. The limit state sought in this study is collapse. Collapse is assumed to occur if: (a) the Global Index of Damage (GID) proposed by Park and Ang (1985) and Park *et al.* (1987) reaches the value GID=1; or (b) if the maximum

Table 2 Accelerograms used for the dynamic analyses

Wave name	Earthquake	Station	Epicentral distance (km)	Fault distance (km)	Magnitude	PGA (g)
289ya	Campano-Lucano	Mercato San Severino	48	33	6.9 Mw	0.14
170ya	Basso Tirreno	Patti-Cabina Prima	18	13	6.1 Mw	0.16
175ya	Volvi	Thessaloniki-City Hotel	29	13	6.3 Mw	0.15
198xa	Montenegro	Ulcinj-Hotel Albatros	21	11	7.0 Mw	0.18
475xa	Manjil	Abhar	98	82	7.4 Mw	0.13
581xa	Komilion	Lefkada-OTE Building	16	-	5.4 Mw	0.18
665xa	Umbria Marche	Assisi-Stallone	21	14	6.0 Mw	0.19
123xa	Friuli	Forgaria-Cornio	15	16	5.5 Mw	0.13
126xa	Friuli	Breginj-Fabrika IGLI	21	18	6.0 Mw	0.47
134xa	Friuli	Forgaria-Cornio	14	17	6.0 Mw	0.26
139xa	Friuli	Breginj-Fabrika IGLI	25	22	6.0 Mw	0.16
146xa	Friuli	Forgaria-Cornio	14	17	6.0 Mw	0.35
147xa	Friuli	San Rocco	14	17	6.0 Mw	0.14
229xa	Montenegro	Petrovac-Hotel Oliva	25	17	6.2 Mw	0.17
1313xa	Ano Liosia	Athens 3 - Kallithea	16	16	6.0 Mw	0.27
2015xa	Kefallinia	Argostoli-OTE Building	18	18	6.2 Mw	0.18

peak interstory drift exceeds 1.5% of the story height. Regarding the first criterion, Park *et al.* (1987) calibrated the GID index with respect to the observed damage of nine reinforced concrete buildings damaged during the 1971 San Fernando and the 1978 Miyagiken-oki earthquakes and concluded that GID $\geq 1$  represents collapse. As for the second criteria, interstory drifts larger than 1.5% have been associated with collapse in past studies on existing gravity-load designed RC frames (Masi 2004). This ultimate drift of 1.5% is based on indications drawn in the literature for structures not designed with antiseismic criteria (Park and Ang 1985, Naeim 1989, Kunnath *et al.* 1990, Ghobarah *et al.* 1999). In all the analyses conducted for this study, collapse was triggered by the shear failure of columns: i.e., when the ultimate state was attained, one or two plastic hinges in columns had reached their ultimate curvature ductility capacity. In a real frame, the shear failure of a column is likely to be associated with loss of its gravity load capacity, and this can result in total collapse of the building. Also, in all the cases analyzed, the shear failure of a column was preceded by the formation of plastic hinges at the top and/or bottom of the columns of the same story, combined with plastic hinges at the ends of the upper and/or lower beams of the story. In contrast to the shear failure of a column, the exceedance of the ultimate curvature ductility capacity in a single or several beams of a given story does not necessarily jeopardize the structural integrity of the whole building.

### 3. Definition of energy response parameters

In this study, the seismic capacity of the frames is evaluated in terms of the total amount of input energy and hysteretic energy that they can absorb/dissipate until collapse. Appropriate energy response parameters are defined below from the dynamic equilibrium conditions of a multi-degree-of-freedom (MDOF) system, given by the following matrix differential equation

$$\mathbf{M}\ddot{\mathbf{y}}(t) + \mathbf{C}\dot{\mathbf{y}}(t) + \mathbf{Q}(t) = -\mathbf{M}\mathbf{r}\ddot{z}_g(t) \quad (2)$$

Here  $\mathbf{M}$  and  $\mathbf{C}$  are the mass and damping matrices respectively;  $\mathbf{Q}(t)$  is the restoring force vector;  $\ddot{\mathbf{y}}(t)$  and  $\dot{\mathbf{y}}(t)$  are, respectively, the acceleration and velocity vectors relative to the ground;  $\mathbf{r}$  is the influence coefficient vector which represents the displacement vector,  $\mathbf{y}(t)$ , resulting from a unit support displacement; and  $\ddot{z}_g(t)$  is the acceleration of the input ground motion. Multiplying Eq. (2) by  $d\mathbf{y} = \dot{\mathbf{y}}(t)dt$  and integrating over the entire duration of the earthquake, i.e., from  $t=0$  to  $t=t_0$ , it reduces to

$$E_k + E_\xi + E_a = E \quad (3)$$

$$E_k = \int_0^{t_0} \dot{\mathbf{y}}^T \mathbf{M} \ddot{\mathbf{y}} dt; \quad E_\xi = \int_0^{t_0} \dot{\mathbf{y}}^T \mathbf{C} \dot{\mathbf{y}} dt; \quad E_a = \int_0^{t_0} \dot{\mathbf{y}}^T \mathbf{Q} dt; \quad E = - \int_0^{t_0} \dot{\mathbf{y}}^T \mathbf{M} \mathbf{r} \ddot{z}_g dt \quad (4)$$

$E_k$  is the kinetic energy at the instant when shaking ends;  $E_\xi$  is the energy dissipated by the inherent damping;  $E_a$  is the absorbed energy; and  $E$  is, by definition, the seismic input energy.  $E_a$  is composed of the recoverable elastic strain energy,  $E_s$ , and the irrecoverable hysteretic energy  $E_h$ , i.e.,  $E_a = E_s + E_h$ ; thus Eq. (4) is rewritten

$$E_k + E_\xi + E_s + E_h = E \quad (5)$$

Further,  $E_h$  is the sum of hysteretic energy  $E_{hi}$  dissipated by each story  $i$ , i.e.,  $E_h = \sum_{i=1}^N E_{hi}$ . The left hand side of Eq. (5) can be interpreted as the seismic capacity of the structure, while the right hand side represents the earthquake loading effect in terms of input energy (Housner 1956, Akiyama 1985). Past research (Zahrah and Hall 1984, Akiyama 1985, Kuwamura and Galambos 1989) has shown that in general MDOF systems: (i)  $E$  is only mildly affected by the strength and by the configuration of the restoring force characteristics of the structure; (ii)  $E$  is scarcely affected by the fraction of critical damping  $\xi$ ; (iii)  $E/M_T$  is independent of the total mass  $M_T$  of the structure; and (iv)  $E/M_T$  is governed by the first vibration mode. Recalling Eq. (5),  $E_e = E_k + E_s$  is the elastic strain energy, and  $E_D = E - E_\xi$  is the so-called energy contributable to damage; thus Eq. (5) can be rewritten as follows

$$E_e + E_h = E_D \quad (6)$$

For convenience,  $E$  and  $E_D$  can be expressed in terms of equivalent velocities,  $V_E$  and  $V_D$ , by

$$V_E = \sqrt{2E/M_T}; \quad V_D = \sqrt{2E_D/M_T} \quad (7)$$

The condition for the building surviving the earthquake is  $(E_e + E_\xi + E_h) \geq E$ . In damped systems the elastic strain energy  $E_e$  at the end of the earthquake is almost zero; this fact is enhanced in the case of nonlinear behavior. Therefore, recalling Eq. (6),  $E_D$  is approximately equal to  $E_h$ , and  $V_D$  can be interpreted as the total hysteretic energy dissipated by the system at the end of the ground motion, expressed in terms of an equivalent velocity.

## 4. Results of the non-linear dynamic response analyses

### 4.1 Hysteretic energy $E_{hi}$ dissipated by each story

The hysteretic energy dissipated by each story during the cyclic reversals imposed by earthquake  $E_{hi}$  can be expressed in non-dimensional form in terms of a parameter  $\eta_i$  defined as

$$\eta_i = \frac{E_{hi}}{Q_{yi}\delta_{yi}} \quad (8)$$

If the ratio  $\eta_i$  is computed at the instant of collapse of the story, it represents its ultimate hysteretic energy dissipation capacity  $\eta_{u,i}$ . The  $\eta_{u,i}$  of the story that first reached its ultimate capacity was determined from the results of the non-linear dynamic response analyses. The story was considered to collapse when the Story Index of Damage (SID) proposed by Park and Ang (1985) and Park *et al.* (1987) reached the value SID=1; or (b) when the interstory drift reached 1.5% of the story height. Fig. 4 shows the resulting values of  $\eta_{u,i}$ , which range from 0.5 to 4 depending on the frame and the acceleration record used. The mean value of  $\eta_{u,i}$  is 1.32, with a coefficient of variation (ratio between the standard deviation and the mean) of 0.62. These values are noticeably below those found, for example, in RC frames with normal beams designed with the strong column-weak for which  $\eta_{u,i}$  is typically larger than 17. This reference value (i.e.,  $\eta_{u,i}=17$ ) has been determined from the extensive experimental studies of well-behaving non-wide beam-column connections investigated by Darwin and Nmai (1986).

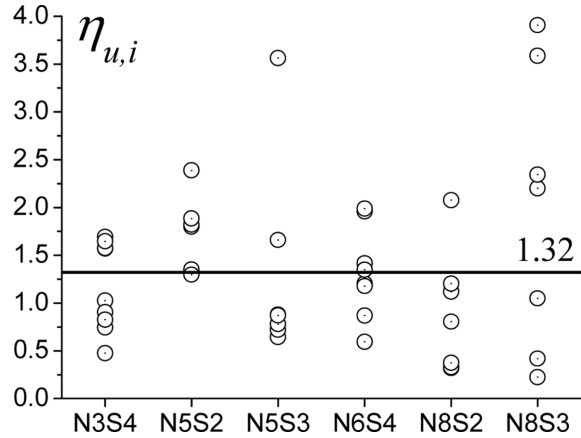


Fig. 4 Normalized hysteretic energy dissipated by the collapsing story

#### 4.2 Distribution of hysteretic energy $E_{hi}$ among the stories

The ultimate seismic capacity of the overall building does not depend only on the  $\eta_{u,i}$  of each story; it is also influenced by how the hysteretic energy is distributed among the stories. Hysteretic energy concentration (i.e., damage concentration) in a given story can jeopardize the ultimate energy dissipation capacity of the overall structure. Therefore, investigating the proneness of a given structural type to damage concentration is a matter of prime importance in the seismic evaluation of existing frames. Fig. 5 shows the distribution of hysteretic energy  $E_{hi}/E_h$  among the stories of the analyzed frames under the records of Table 2 – not all records are drawn in each graph for the sake of clarity. The hysteretic energies are calculated at collapse. Although the  $E_{hi}/E_h$  distribution varies from one record to another, a trend is observed, with  $E_{hi}$  concentrating in certain stories. For example, in frame N5S2 the hysteretic energy tends to concentrate in the fourth story, while in models N8S2 and N8S3 this tendency is observed towards the seventh and eighth stories. It is also worth noting that in the story where the hysteretic energy concentrates, the ratio  $E_{hi}/E_h$  is close to the largest attainable value  $E_{hi}/E_h=1$ . This fact underlines that, for the structural typology under study, the possibility that at collapse most hysteretic energy concentrates in a single story – i.e., severe damage concentration – is a matter of prime importance.

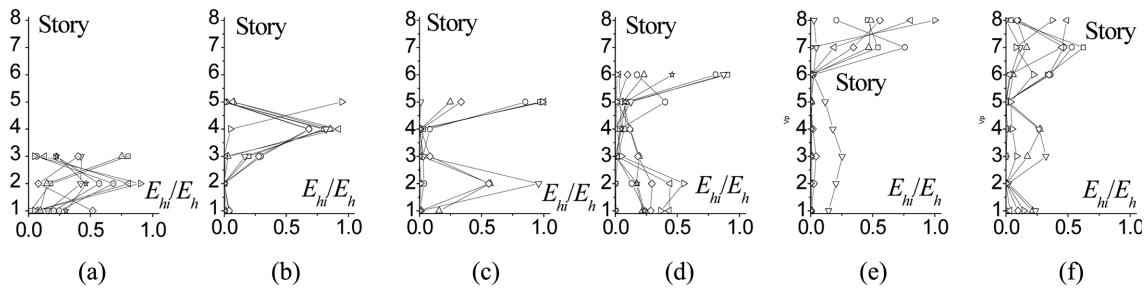


Fig. 5 Hysteretic energy distributions of frames (a)N3S4, (b)N5S2, (c)N5S3, (d)N6S4, (e)N8S2, (f)N8S3

#### 4.3 Relation between hysteretic energy consumption under cyclic and monotonic loading

Fig. 6 shows the typical story shear-interstory drift curve,  $Q_i-\delta_i$ , of a given story  $i$  of a building subjected to seismic-type cyclic loading.  $Q_{yi}$  and  $\delta_{yi}$  are the corresponding values at yielding. By integrating this  $Q_i-\delta_i$  curve, the hysteretic energy dissipated by the  $i$ -th story,  $E_{hi}$ , is obtained. From the  $Q_i-\delta_i$  plot, the envelope curve in the positive and negative domains can be drawn, as indicated with bold lines in Fig. 6. The largest and smallest areas delimited by the envelope curve in each domain of deformation will be denoted by  $E_{hm,i}^{max}$  and  $E_{hm,i}^{min}$ ; they represent the plastic strain energy that story  $i$  would dissipate in each domain if the load were applied monotonically up to the maximum interstory drifts  $|\delta_{max,i}|$ ,  $|\delta_{min,i}|$ . Now, the averaged,  $\bar{E}_{hm,i}$ , and the total,  $E_{hm,i}$ , plastic strain energies under monotonic loading are defined by

$$\bar{E}_{hm,i} = \frac{(E_{hm,i}^{max} + E_{hm,i}^{min})}{2}; \quad E_{hm,i} = E_{hm,i}^{max} + E_{hm,i}^{min} \quad (9)$$

From  $\bar{E}_{hm,i}$  and  $E_{hm,i}$  two new ratios  $a_{pi}$  and  $b_{pi}$  are defined for each story

$$a_{pi} = \frac{E_{hi}}{\bar{E}_{hm,i}}; \quad b_{pi} = \frac{\bar{E}_{hm,i}}{E_{hm,i}^{max}} \quad (10)$$

For given fixed values of  $|\delta_{max,i}|$  and  $|\delta_{min,i}|$ ,  $a_{pi}$  represents the increase in hysteretic energy due to cyclic reversals of deformation with respect to the value that would be obtained by applying the load monotonically. The larger  $a_{pi}$  is, the greater the efficiency of the frame in dissipating energy with respect to the maximum deformation. Meanwhile,  $b_{pi}$  measures the extent to which the plastic strain deformation biases towards the positive or negative domain. By definition  $b_{pi}$  is in the range  $0.5 \leq b_{pi} \leq 1$ . Fig. 7 shows the relations  $E_{hi}$  vs.  $E_{hm,i}$ , and  $\bar{E}_{hm,i}$  vs.  $E_{hm,i}^{max}$  for the frames analyzed at the instant when they reached their ultimate state. A linear regression of these points  $(E_{hi}, E_{hm,i})$  and  $(\bar{E}_{hm,i}, E_{hm,i}^{max})$  gives  $a_{pi}=1.6$  and  $b_{pi}=0.76$ , with respective standard errors of 0.058 and 0.007. These values of  $a_{pi}$  and  $b_{pi}$  are close to those obtained in past studies (Benavent-Climent *et al.* 2004) for

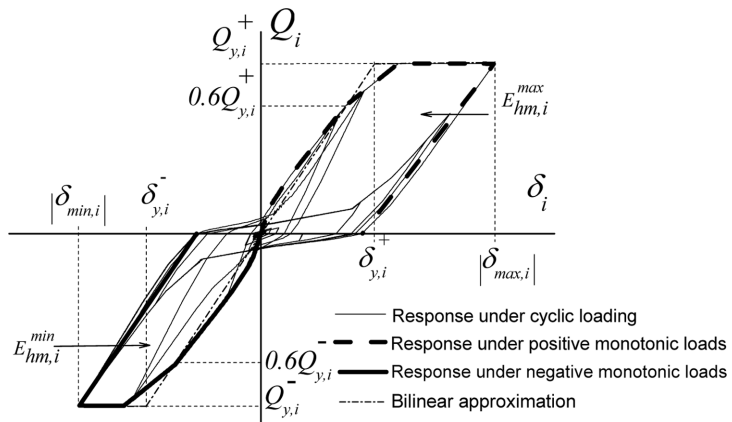


Fig. 6 Story shear-interstory drift curve of a given story

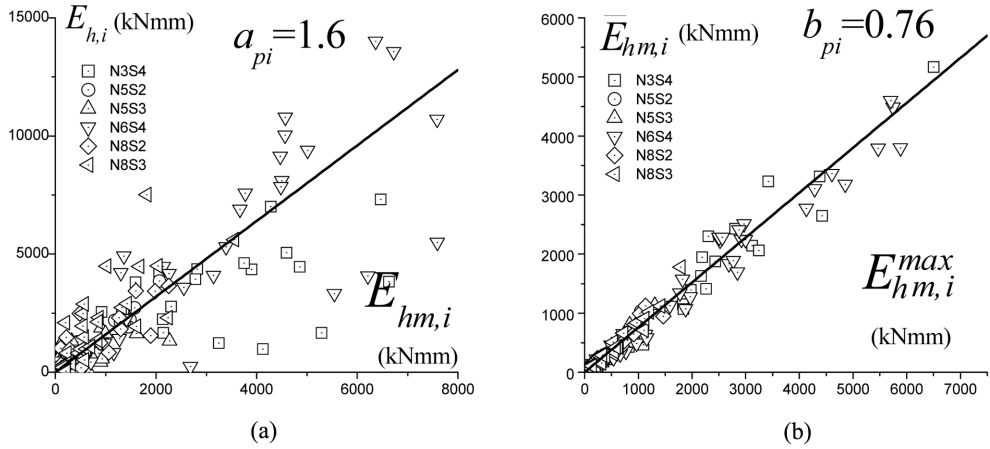


Fig. 7 Hysteretic energy consumption under cyclic and monotonic loading (a)  $E_{hi}$  vs  $E_{hm,i}$ , (b)  $\bar{E}_{hm,i}$  vs.  $E_{hm,i}^{max}$

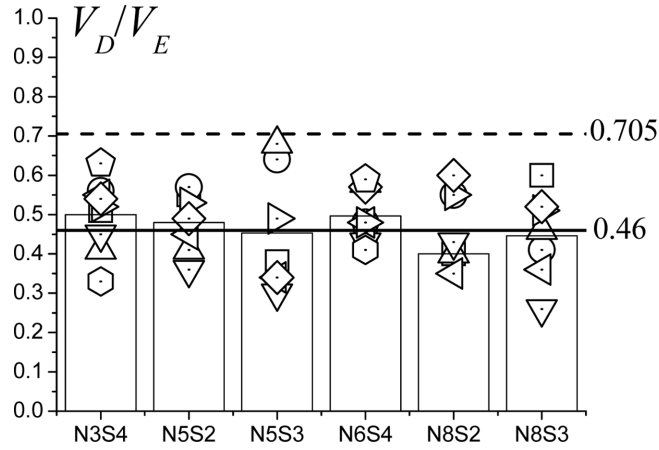
general existing gravity-load designed RC buildings ( $a_{pi}=1.5$  and  $b_{pi}=0.75$ ). The obtained value of  $b_{pi}$  is halfway between the limits 0.5-1, indicating that the plastic deformations do not develop by equal amounts in both domains of displacement. As for the value  $a_{pi}=1.6$ , it is rather low in comparison with the average (2.5) reported by Akiyama (1999) for RC frames with non-wide beams designed with standard details and adequate antiseismic criteria. This would indicate that the efficiency of the old RC frames with wide beams in dissipating hysteretic energy – as measured by parameter  $a_{pi}$  – is about 2/3 that of the RC frames with normal beams designed as prescribed by modern codes.

#### 4.4 Relation between hysteretic energy and total dissipated energy

Fig. 8 shows the ratio  $V_D/V_E$  between the energy contributable to damage  $E_D$  and the total energy input by the earthquake  $E$  at collapse, both expressed in terms of the equivalent velocities  $V_D$  and  $V_E$  defined by Eq. (7). The symbols represent the response under each ground motion, and the column bars the mean value for each frame. The ratio  $V_D/V_E$  averaged for each frame ranges from 0.4 to 0.5, and the mean value is 0.46, as indicated by the solid line. Also shown in Fig. 8 with a solid line is the  $V_D/V_E = 0.705$  predicted using Akiyama's equation (Akiyama 1985) for  $\xi=5\%$  of critical damping, which is noticeably larger – i.e., on the safe side – than the value computed for the structural typology under study. The reason of this discrepancy is that Akiyama's equation was obtained for nonlinear systems with high levels of hysteretic energy dissipation capacity – i.e., high levels of  $\eta_{u,i}$ , yet the old RC frames with flat beams investigated in this study exhibit small values of  $\eta_{u,i}$ , as discussed in subsection 4.1. Past research on improving Akiyama's equation has shown (Benavent-Climent *et al.* 2002) that, for a fixed  $\xi$ , the ratio  $V_D/V_E$  varies according to the following law

$$V_D/V_E = \frac{1.15\eta}{0.75 + \eta} \left( \frac{1}{1 + 3\xi + 1.2\sqrt{\xi}} \right) \quad (10)$$

where  $\eta$  is the maximum value of  $\eta_{u,i}$  among the stories. Making  $V_D/V_E=0.46$  and  $\xi=0.05$  in Eq.

Fig. 8 Relation between  $V_D$  and  $V_E$ 

(10), and solving for  $\eta$  gives  $\eta=1$ . This value  $\eta=1$  is very close to that exhibited by the analyzed frames at the ultimate state ( $\eta_{u,i}=1.36$ ); so that the appropriateness of Eq. (10) for the structural typology under study is confirmed.

#### 4.5 Ultimate energy dissipation capacity and comparison with energy dissipation demand

Fig. 9 shows the energy contributable to damage  $E_D$  and the total energy input by the earthquake  $E$  expressed in terms of the equivalent velocities  $V_D$  and  $V_E$ . For each frame indicated in the abscissa, the symbols represent the response under each ground motion, and the column bar the mean for each frame. In most cases the  $V_D$  and  $V_E$  obtained for a given frame under different records are quite close to the mean – the coefficients of variation range from 0.09 to 0.3. According to past research (Benavent-Climent *et al.* 2002), the energy dissipation demand in the southern part of Spain (Granada region) – considering stiff soil and the design PGA=0.23g prescribed by the

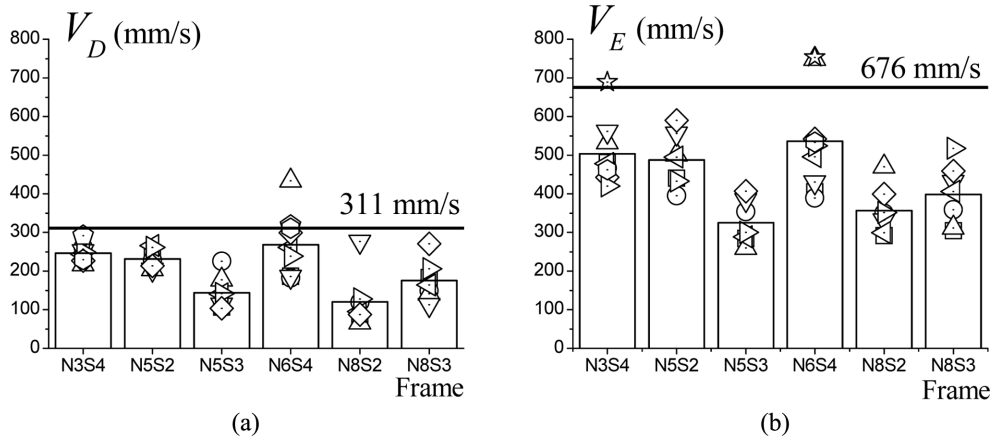


Fig. 9 Ultimate energy dissipation capacity (a) hysteretic energy, (b) total input energy

current seismic code – is 676 mm/s, as indicated by the solid horizontal line in Fig. 9(b). The analyzed frames exhibit mean values of  $V_E$  ranging from 325 mm/s to 535 mm/s. This means that the ultimate energy dissipation capacity of the analyzed frames in terms of equivalent velocity ranges from 1/2 to 3/4 of the value required for surviving the design earthquake. If the comparison is made directly in terms of input energy  $E$ , the seismic capacity ranges from  $(1/2)^2 \approx 1/4$  to  $(3/4)^2 \approx 1/2$  of the seismic demand.

As for the energy contributable to damage, the  $V_D$  averaged for each frame ranges from 120 mm/s to 246 mm/s. Assuming that the ratio  $V_D/V_E$  for the structural typology under study is 0.46 (as discussed in subsection 4.4), the expected hysteretic energy demand in terms of equivalent velocity for these frames in the southern part of Spain (Granada region) is  $0.46 \times 676 = 311$  mm/s. This means that the hysteretic energy dissipation capacity of the analyzed frames is far below the expected demand – i.e., between  $(120/311)^2 = 0.15$  and  $(246/311)^2 = 0.62$ . It is determined, thus, that the analyzed frames have a high level of vulnerability and should be seismically upgraded.

## **6. Conclusions**

A numerical study was conducted to investigate the seismic performance of existing reinforced concrete frames with wide beams designed mainly for gravity loads, as typically found in the seismic-prone Mediterranean area. This type of frame was built before the introduction of modern seismic codes, and their safety in the event of a severe earthquake is a matter of great concern. Six plane frames representative of past construction practices in the southern part of Spain were designed, and the corresponding non-linear numerical models were developed using the results of previous tests. The seismic response until the frames reached their ultimate collapse state was obtained by applying the incremental non-linear dynamic analysis method, and expressed in terms of energy dissipation demands. The following conclusions can be drawn:

- (1) The ultimate energy dissipation capacity at the story level ranges from about 0.5 to 4 times the product of the lateral yield strength and yield displacement of the story, the mean being 1.36. This value is smaller than that reported for well designed RC frames with normal beams.
- (2) The structural typology investigated is very prone to concentrate most hysteretic energy (damage) in a single story, which jeopardizes the seismic capacity of the overall frame.
- (3) The efficiency in dissipating hysteretic energy is about 2/3 of that of the RC frames with normal beams designed as prescribed by modern codes.
- (4) The fraction of the total input energy that must be dissipated through plastic deformations by beams and columns – i.e., hysteretic energy – is about  $0.46^2 = 0.21$  times the total energy input by the earthquake.
- (5) The ultimate total energy dissipation capacity ranges from 1/4 to 1/2 of the seismic demand – earthquake input energy – expected at the site of location. The hysteretic energy dissipation capacity is also far below the expected demand.

This study is based in 2D frames; however, buildings are 3D in nature. Stiffness or mass asymmetries can result in very complex torsional responses that make the dynamic behavior nearly unpredictable. Further work is needed to address this key issue.

## Acknowledgements

This research was funded by the Spanish Ministry of Education and Science (project BIA2005-00591) and by the European Union (*Fonds Européen de Développement Régional*).

## References

- Akiyama, H. (1985), *Earthquake Resistant Limit-State for Buildings*, University of Tokyo Press, Tokyo.
- Akiyama, H. (1999), *Energy-based design method for buildings based on energy balance*, Gihodo Shuppan Co., Tokyo (in Japanese).
- Ambraseys, N.N., Douglas, J., Sibjörnsson, R., Berge-Thierry, C., Suhadolc, P., Costa, G. and Smith, P.M. (2004), *Dissemination of European Strong-Motion Data*, Vol. 2, CD ROM Collection, Engineering and Physical Sciences Research Council, United Kingdom.
- Aycardi, L.E., Mander, J.B. and Reinhorn, A.M. (1994), "Seismic resistance of R.C. frame structures designed only for gravity loads: Experimental performance of subassemblages", *ACI Struct. J.*, **91**(5), 552-563.
- Benavent-Climent, A., (2005), "Shaking table tests of reinforced concrete wide beam-column connections", *Earthq. Eng. Struct. D.*, **34**, 1833-1839.
- Benavent-Climent, A. (2007), "Seismic behavior of RC wide beam-column connections under dynamic loading", *J. Earthq. Eng.*, **11**, 493-511.
- Benavent-Climent, A., Cahis, X. and Zahran, R. (2009a), "Exterior wide beam-column connections in existing RC frames subjected to lateral earthquake loads", *Eng. Struct.*, **31**, 1414-1424.
- Benavent-Climent, A., Akiyama, H., López-Almansa, F. and Pujades, L.G. (2004), "Prediction of ultimate earthquake resistance of gravity-load designed RC buildings", *Eng. Struct.*, **26**, 1103-1113.
- Benavent-Climent, A., Cahis, X. and Vico, J.M. (2009b), "Interior wide beam-column connections in existing RC frames subjected to lateral earthquake loading", *Bull. Earthq. Eng.*, DOI 10.1007/s10518-009-9144-3.
- Benavent-Climent, A., Pujades, L.G. and Lopez-Almansa, F. (2002), "Design energy input spectra for moderate seismicity regions", *Earthq. Eng. Struct. D.*, **31**, 1151-1172.
- Beres, A., Pessiki, S., White, R. and Gergely, P. (1996), "Implications of experimental on the seismic behaviour of gravity load designed RC beam-column connections", *Earthq. Spectra*, **12**(2), 185-198.
- Li, B., Wu, Y.M. and Pan, T.C. (2002), "Seismic behaviour of non-seismically detailed interior beam-wide column joints. Part I: Experimental results and observed behaviour", *ACI Struct. J.*, **99**(6), 950-977.
- Calvi, G.M., Magenes, G. and Pampanin, S. (2002), "Relevance of beam-column damage and collapse in RC frame assessment", *J. Earthq. Eng.*, **6**(2), 75-100.
- Darwin, D. and Nmai, C.K. (1986), "Energy dissipation in RC beams under cyclic load", *J Struct. Eng.*, **112**(8), 1829-1846
- Ghobarah, A., Abou-Elfath, H. and Biddah, A. (1999), "Response based damage assessment of structures", *Earthq. Eng. Struct. D.*, **78**, 789-1104.
- Hakuto, S., Park, R. and Tanaka, H. (2000), "Seismic Load Tests on Interior and Exterior Beam Column Joints with Substandard Reinforcing Details", *ACI Struct. J.*, **97**(1), 11-25.
- Housner, G.W. (1956), "Limit design of structures to resist earthquakes", *Proceedings of the 1st World Conference on Earthquake Engineering*, Berkeley, CA.
- Kunnath, S.K., Mander, J.B. and Reinhorn, A.M. (1990), "Seismic response and damageability of gravity-load (non-seismic) designed buildings", *Proceeding of 9th European Conference on Earthquake Engineering*, Moscow.
- Kuwamura, H. and Galambos, T.V. (1989), "Earthquake load for structural reliability", *J. Struct. Eng.*, **115**(6), 1446-1462.
- Masi, A. (2004), "Seismic vulnerability assessment of gravity load designed R/C frames", *Bull. Earthq. Eng.*, **1**(1), 371-395.
- Naeim, F. (1989), *The seismic design handbook*, Van Nostrand Reinhold, New York.
- Park, R. (2002), "A summary of results of simulated seismic load tests on reinforced concrete beam-column

- joints, beams and columns with substandard reinforcing details”, *J. Earthq. Eng.*, **6**(2), 1-27.
- Park, Y.J. and Ang, A.H.S. (1985), “Mechanistic seismic damage model for reinforced concrete”, *J. Struct. Eng.*, **111**(4), 722-739.
- Park, Y.J., Ang, M. and Wen, Y.K. (1987), “Damage-limiting aseismic design of buildings”, *Earthq. Spectra*, **3**(1), 1-26.
- Park, Y.J., Reinhorn, A.M. and Kunnath, S.K. (1987), “IDARC: Inelastic Damage Analysis of Reinforced Concrete Frame-Shear Wall Structures”, Technical Report NCEER-87-0008, New York.
- Priestley, M.J.N. (1997), “Displacement-based seismic assessment of reinforced concrete buildings”, *J. Earthq. Eng.*, **1**(1), 157-192.
- Sezen, H. and Mohele, P. (2006), “Seismic tests of concrete columns with light transverse reinforcement”, *ACI Struct. J.*, **103**(6), 842-49.
- Sivaselvan, M.V. and Reinhorn, A.M. (1999), “Hysteretic models for cyclic behavior of deteriorating inelastic structures”, Technical Report NCEER-99-0018, New York.
- Sugano, S. (1968), “Study on inelastic stiffness of reinforced concrete structures”, Reports of the Annual Meeting, Architectural Institute of Japan Kanto, Tokyo (in Japanese).
- Vamvatsikos, D. and Cornell, C.A. (2002), “Incremental dynamic analysis”, *Earthq. Eng. Struct. D.*, **31**, 491-514.
- Zahrah, T.F. and Hall, W.J. (1984), “Earthquake energy absorption in SDOF structures”, *J. Struct. Eng.*, **110**(8), 1757-1772.